Environ. Sci. Technol. **2006**, *40,* 6163−6169

On the Mode of Action of *N*-Phenyl-2-naphthylamine in Plants

ROLF ALTENBURGER,*,† WERNER BRACK,† WILLIAM R. GRECO,‡ MATTHIAS GROTE,† KLAUS JUNG,† AGNES OVARI,† JANET RIEDL,† KATRIN SCHWAB,† AND EBERHARD KÜSTER†

UFZ Centre for Environmental Research Leipzig-Halle, Permoserstrasse 15, 04318 Leipzig, Germany, and Roswell Park Cancer Institute, Elm & Carlton Streets, Buffalo, New York 14263

N-phenyl-2-naphthylamine, a sediment contaminant previously identified as a major toxicant of site-specific importance was investigated for its mode of toxic action. From short-term bioassays with daphnids, fish eggs, bacteria, and algae it appears that this compound has specific phytotoxic properties at concentrations below 100 μg/L, which cannot be explained assuming an unspecific narcosis type of action in plants. Also, hydroxy-, nitro-, and methyl-derivatives show clear excess toxicity as compared to baseline toxic effects. Of several plant-specific growth and development processes investigated, only photosynthesis could be demonstrated to be affected at short exposure times and low concentrations. Disturbance of primary photosynthetic reactions such as oxygen evolution and fluorescence quenching, however, becomes only apparent after 2−3 h of exposure, which is in sharp contrast to known specific inhibitors targeting processes such as electron transport or ATP production. This, and concentration-time-effect modeling lead to the suggestion that *N*-phenyl-2-naphthylamine acts intracellular as a reactive compound in cell membranes producing irreversible, and thus cumulative, damage over time in algae. The effects may become first apparent in membrane-rich compartments such as the algal chloroplast.

Introduction

N-phenyl-2-naphthylamine (PNA) has been identified as a major contaminant occurring in riverine sediments of the Spittelwasser, a tributary to the Elbe river. PNA exhibits an unexpected potential for toxic effects in aquatic organisms (*1*). It has been used as a stabilizer for organic polymers. Furthermore, it is formed as a byproduct in the production of *N*-phenyl-1-naphthylamine, and as an additive to jet oils (*2*). Commonly, considerations focus on *N*-phenyl-1-naphthylamine, where the production volume is known to have been between 1000 and 1500 t/a (*3*). This compound has been evaluated as a priority compound by ref *3*. *N*-phenyl-naphthylamine has been detected in sediments and freshwater in the proximity of chemical production sites in mg/kg and μg/L concentrations (*1*, *4*, *5*). Due to its lipophilicity (octanol−water partition coefficient, log K_{OW} of 4.2) it is regarded to have a considerable bioaccumulative potential in aquatic environments. However, there are no data available as to its biodegradation in sediments (*3*, *6*).

Regarding the toxicological potency for *N*-phenyl-1-naphthylamine, acute as well as subchronic animal studies demonstrated effects from dosages above 1000 mg/kg body weight (*2*, *3*). In vertebrates it is readily absorbed, converted to metabolites and excreted. Indication of carcinogenicity of PNA in mice was reported (*7*) but the findings have been challenged (*3*). Ecotoxic effects have been reviewed as being in the mg/L range for acute toxicity in rainbow trout (*Oncorhynchus mykiss*) and bluegill sunfish (*Lepomis macrochirus*), in embryo development studies using clawed frog (*Xenopus laevis*), and in inhibition of cell proliferation of the freshwater ciliates *Tetrahymena pyriformis* and in acute testing using *Daphnia magna* (*3*). Biochemical studies have reported malformations in *Xenopus laevis* larvae, which again take place in concentrations from 1−4 mg/L after 48 h of exposure, as described by Greenhouse (*8*).

Our initial findings investigating sediment extracts with multiple contaminants (*1*) suggested an unprecedented algal toxicity with effects at concentrations comparable to specifically acting herbicides. Furthermore, it was demonstrated that PNA contributes to the combined effects of mixtures occurring at specific sites (*9*). The objectives of this investigation, therefore, were to unravel whether PNA exhibits a specific mode of action in plants and possibly identify processes or plant-specific targets. Mode of action knowledge is needed when attempting to assess effective exposures and potential mixture toxicity from complex contamination, but it is also required as a basis for extrapolating to other organisms.

Materials and Methods

Chemicals. Specifications for *N*-phenyl-2-naphthylamine (PNA) and the derivatives used regarding source, purity, and water solubility can be found in the Supporting Information. N-(3-nitrophenyl)-2-naphthylamine (PNA-NO_2) and N-(4-methylphenyl)-2-naphthylamine (PNA-pCH_3) were synthesized. All other chemicals were at least of pro analysis quality from major chemical distributors. All experiments were carried out using an organic stock solution in DMSO, applying PNA with DMSO as a cosolvent checked with solvent negative controls.

Bioassays. Short-term inhibition of luminescence of the gram-positive bacterium *Vibrio fischeri* after 15 and 30 min of exposure was detected according to ref *11*. Immobilization of neonates of *Daphnia magna* was observed according to ref *12* but modified for the test medium (*13*). Development of *Danio rerio* fish eggs was followed under conditions specified elsewhere (*14*).

Using the green alga *Desmodesmus subspicatus,* fluorometric quantification (SpectraMax Gemini EM, Molecular Devices, Sunnyvale, U.S.) of chlorophyll a increases as biomass parameter (480 nm excitation, 675 nm emission) after 72 h of growth according to ref *15* was performed, and the test medium was prepared according to ref *9*. Effects on the reproduction of the unicellular green alga *Scendemus vacuolatus* were recorded applying a protocol specified earlier (*9*). The same cultivation technique was applied to quantify the effects on cell volume during the cell cycle using an electronic cell analyzer (CASYII, Schärfe Systems, Reutlingen, Germany). Photosynthetic oxygen production of *S. vacuolatus* was determined with a Clark-type electrode. Pulse amplitude modulated fluorescence quenching analysis of chlorophyll a, measured at 680 nm using a PAM fluorometer (Water PAM,

* Corresponding author e-mail: rolf.altenburger@ufz.de; phone: +49.341.235.2224; fax: +49.341.235.2401.
† UFZ Centre for Environmental Research.
‡ Roswell Park Cancer Institute.

10.1021/es060338e CCC: $33.50
Published on Web 09/06/2006

TABLE 1. Concentration Effect Functions, Median Effects, and Calculated Excess Toxicity for *N*-Phenyl-2-Naphthylamine and Derivatives in Various Organism Bioassays[a]

compound	log K_{ow}[b]	bioassay	Hill parameters[c] θ_1, EC_{50} [μg/L] [CI 95%]	Hill parameters[c] θ_2, slope	baseline toxicity modeled EC_{50} [μg/L]	excess toxicity EC_{50}-ratio expected/observed
N-phenyl-2-naphthylamine (PNA)	4.47	*Daphnia magna*, mobility, 48 hrs	30.6 [21.5, 39.7]	1.70	3620[e]	12
		Vibrio fischeri, autoluminescence, 30 min	165[d]	0.725	2000[f]	1.0[d]
		Desmodesmus subspicatus, population growth, 72 hrs	171 [146, 197]	3.17	9750[g]	57
		Scenedesmus vacuolatus, cell reproduction, 24 hrs	33.5 [31.9, 35.0]	6.68	6600[h]	200
		Danio rerio, egg development, 48 hrs	313 [300, 327]	4.07	3780[i]	12
N-(4-hydroxyphenyl)-2-naphthylamine (PNA-OH)	3.68	*Scenedesmus vacuolatus*, cell reproduction, 24 hrs	296 [278, 314]	3.87	19900[h]	67
N-(3-nitrophenyl)-2-naphthylamine (PNA-NO_2)	4.86	*Scenedesmus vacuolatus*, cell reproduction, 24 hrs	16.7 [16.0, 17.3]	5.87	2140[h]	130
N-(4-methylphenyl)-2-naphthylamine (PNA-pCH_3)	5.01	*Scenedesmus vacuolatus*, cell reproduction, 24 hrs	69.7 [65.3, 74.2]	5.23	1400[h]	20

[a] CI approximated 95% confidence interval, n.a. not available. [b] Estimated using kowWin Vers. 1.66 (*10*). [c] Estimated fitting the following nonlinear model to the normalized observations (E): $E = \theta_3/((1 + (conc/\theta_1)^{-\theta_2})$ with conc. signifying the concentrations in μg/L, and θ_3 fixed at 1, except for *Vibrio fischeri*. [d] An amount of 2000 μg/L gives 37% effect in the bacterial assay, the maximum effect observed was 43%, as derived from the Hill parameter θ_3. [e] From ref *25*. [f] From ref *26*. [g] From ref *22*. [h] From ref *9*. [i] Compared to a QSAR for 48 hours lethality in *Pimephales promelas*, (*27*).

Walz GmbH, Effeltrich, Germany) was performed with synchronized cell suspensions of *S. vacuolatus* according to a protocol published previously (*9*) using cells from cell cycle time 14 h. Pollen tube growth of tobacco plants (*Nicotiana sylvestris*) was performed as reported previously (*16*). Cress seeds (*Lapidum sativum*) were used to assay potential inhibition of seed germination and root elongation. A stable isotope ^{15}N-nitrogen test (ESIMA, ecotoxicological stable isotope metabolic assay) was used to study effects on plant nitrogen metabolism according to ref *17*. More detailed descriptions of the bioassays used can be found in the Supporting Information.

Concentration-Effect Relationships and Concentration-Time-Effect Models. Estimation of concentration-effect relationships and concentration-time-effect functions was based on nonlinear regression (*18*) performed in SAS (*19*). The modeling of time-dependent effects (*20*, *21*) required additional values for the bioconcentration factor for PNA, which was estimated using ref *10*.

Results and Discussion

Ecotoxicity or Phytotoxicity. Aquatic organisms of different physiology, namely *Daphnia magna*, *Vibrio fischeri*, *Desmodesmus subspicatus*, *Scenedesmus vacuolatus*, and *Danio rerio* embryos were exposed to *N*-phenyl-2-naphthylamine under short-term exposure of 0.5−72 h duration in serial dilution series. The responses observed showed decreases of activity of the organisms with increasing concentrations. The normalized responses transformed into effects were then used for a nonlinear regression analysis to estimate the parameters of a Hill type concentration-effect relationship (*9*) for each bioassay. All effects monotically increased with concentration. All but the function for the effects on bacteria (parameter values are displayed in Table 1) were found to require only two parameters as an adequate structural pharmacodynamic model for the concentration-effect relationship of PNA in these bioassays. For the results obtained with *Vibrio fischeri*, we assume that no maximum effect was obtained due to solubility problems encountered in the high salt medium. The effective concentrations, illustrated in Table 1 as EC_{50} with approximated 95% confidence values are described rather precisely with a typical deviation of the 95% limit from the EC_{50} estimate of less than 20% and only for the daphnia case with a deviation of almost 100%. The efficacy ranges from 0.313 mg/L for the fish egg assay to 0.0335 mg/L for the algal reproduction assay at the displayed EC_{50} level. As the different bioassays not only differ concerning the effect quality but also with respect to their incubation conditions, confounding effects resulting from these may occur. However, no correlation to the differences in exposure duration times for the different bioassays, which could account for the observed differences in efficacy, can be discerned. The steepness of the concentration−response curves may be deduced from the parameter θ_2. The slope values derived lie between 3 and 7, clearly indicating steeper curves than expected from the law of mass action, which would result in a θ_2 value of 1 in the Hill model, again with the exception of the daphnia and bacteria findings, which provided slopes in that range. These deviations indicate rate-modifying kinetic or dynamic processes. To assess whether the found differences in effective concentrations of PNA between the different species are due to differences in uptake and metabolism (pharmacokinetics) or may be explained by different processes translating primary biochemical interaction into organism response (pharmacodynamics), we used published quantitative structure−activity relationships (QSAR) for calculating an expected concentration for baseline toxicity. Baseline toxicity is regarded as a minimum toxicity that any organic structure exerts at a certain dose, which is only dependent on the lipophilicity of the compound (*22*). Commonly, the octanol−water partition coefficient, logK_{ow}, is taken as a measure of lipophilicity, and we used modeled logK_{ow} estimates here. The anticipated effect is believed to be due to membrane function disturbance and in pharmacodynamic terminology is referred to as narcosis. The excess toxicity, which is the ratio between an effect concentration

necessary to evoke the narcosis type of effects and experimentally determined effect concentration for the same compound (*23*) are also shown in Table 1. Here, it is derived from the ratio of QSAR-based expected narcotic effect and experimentally observed effect concentrations. It quantifies the degree of detected biological activity unexplained by a narcotic mode of action. Evidently, the values for the calculated excess toxicity suggest that PNA is more active than would be expected for a purely unspecific, narcotic mode of action on reproduction of algae only. In contrast, narcosis or polar narcosis (*24*) may suffice to accommodate for the effect concentrations observed in bacteria, daphnia, and fish eggs. Therefore, it might be reasonable to think of a more specific toxicity mechanism in plants.

A second type of experiments was devised to identify whether the found high phytotoxicity is a unique property of PNA or whether structurally similar compounds display similar biological activities. We investigated several PNA derivatives of which the findings for a hydroxy-, a nitro-, and a methyl-derivative of PNA are also summarized in Table 1. The estimated median effect concentrations vary within an order of magnitude while the slopes of the concentration-effect relationships are similar to the one described for PNA in the used algal assay, indicating similar pharmacokinetic properties. However, the calculated excess toxicity shows, that although activities are higher than expected for a purely narcotic type of action, PNA is clearly the most active compound. So, further investigations were focused on PNA.

Interference with Plant-Specific Processes. In order to identify a process in plants that might be prone to specific interference from PNA, a series of experiments was conducted using different bioassays that, in isolation, monitor the functioning of such processes. They may be separated into light-dependent and light-independent processes. Typical plant specific non-light dependent metabolic processes seem to be virtually unaffected by exposure to PNA. Seed germination of watercress was not seriously affected by PNA up to the water solubility limit. Pollen tube growth of tobacco also did not show any sign of adverse effects up to a tested concentration of 10 mg/L. Furthermore, ^{15}N-labeling pattern analysis as monitored by ^{15}N enrichment from nitrate reduction, ammonium assimilation, amino acid, and protein synthesis using the ESIMA assay (*17*) provided no evidence toward an interaction of PNA with plant nitrogen metabolism.

As a double carbon ring system with conjugated bonds and dislocated π-electrons, PNA is capable of absorbing UV light and display fluorescence. This property provoked the idea that indeed phytotoxicity might be attributed to photoenhancement of effects, like it has been shown for PAH compounds (*28*). To test this hypothesis, we followed a protocol established by ref *29* whereby the fluorescent lamps used to provide illumination during photoautotrophic growth of the algae are replaced by a halogen lamp that mimics natural sunlight with a comparatively high proportion of UV light and, alternatively, use this light together with a filter that cuts off all UV irradiance. For the algal bioassay used, complete concentration-effect curves were obtained with no large differences between them. For the test conducted under simulated sunlight, an effect concentration of 57.8 μg/L (95% CI 53.5, 62.0) was obtained which at the EC_{50} level is a factor of 1.7 to achieve the same effect compared to the standard illumination conditions (see Figure A in Supporting Information). The exclusion of UV irradiation from the simulated sunlight lead to a concentration-effect function for PNA that is comparable to that achieved for standard conditions (the EC_{50} was estimated as 34.7 μg/L (95% CI 33.1, 36.3) compared to 33.5 μg/L (95% CI 31.9, 35.0). It might be speculated that the higher EC_{50} observed under simulated sunlight conditions is attributable to photodegradative processes that diminish the PNA concentration during the bioassay. In contrast to UV-absorbing polyaromatic hydrocarbon structures, however, clearly no indication for a photoenhanced effect could be detected.

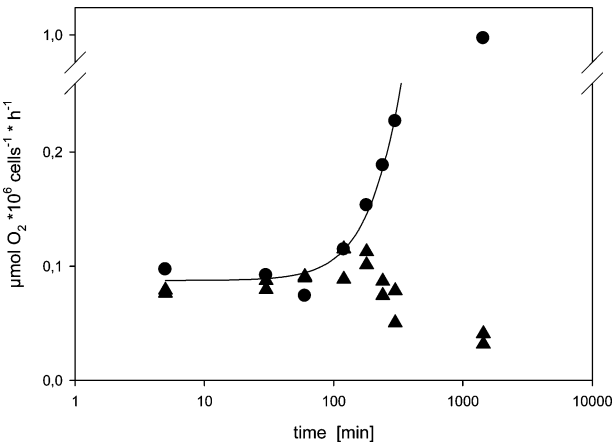

FIGURE 1. Development of photosynthetic oxygen production in *Scenedesmus vacuolatus* exposed to 130 μg/L PNA; control response for the unlimited growth phase can be described as response = log ($y_0 + a \times time^2$), with $y_0 = 1.22$ (representing the initial oxygen production rate of the population), $a = 5.37e^{-6}$ (parameter of increase in oxygen production), and time in min; Circles, untreated control cultures; triangles, cultures exposed to 130 μg/L PNA.

Photosynthesis as the single most prominent light dependent plant growth process was studied using photoautotrophic oxygen production of sub-samples of the same algal cultures of *S. vacuolatus* as before. Several dilution series were run at different exposure durations to identify and quantify effective concentration-time regimes. The experiments required test concentrations high enough to detect effects on a short time scale being indicative of a specific interference. At the same time, concentrations provoking unspecific membrane disturbance had to be avoided. Figure 1 displays the results of a subsequent time-course experiment on the oxygen evolution of an algal suspension under control conditions and when exposed to 130 μg/L of PNA. This concentration is 4 times higher than the median effect concentration for the inhibition of algal reproduction after 24 h exposure, but still 2 orders of magnitude below an expected narcotic effect. While during the first 120 min of observation, no difference between treated and untreated cultures is apparent, subsequently, only the control cultures perform the typical cell cycle increase in oxygen production accounting to a doubling of production rate in 2 h of growth. The PNA-exposed cultures, in contrast, show only a small and delayed increase in O_2-production after 2−3 h, and subsequently, after 5 h of exposure the oxygen production decreases and remains at a low level.

Thus, photosynthesis is affected by PNA exposure at reasonably low concentrations to be considered not due to mere narcosis. The time-lag for the onset of the effect might be attributed to the developing photosynthetic system at early stages in the cell cycle present, though the small but evident increase in photosynthetic oxygen production after 2−3 h indicates differently. In order to clarify this, another kind of experiment was devised using cultures of synchronously grown algae as before but at later points during the cell cycle where the photosynthetic apparatus is fully developed and working at a high rate. In addition, detection of in vivo chlorophyll a fluorescence and analysis of fluorescence quenching parameters (*30*) was employed, to allow higher time resolution and differentiation of different possible targets in the primary photosynthetic reactions. PNA has been reported to form electron donor−acceptor complexes with the naphthoquinone phylloquinone (*31*), which functions

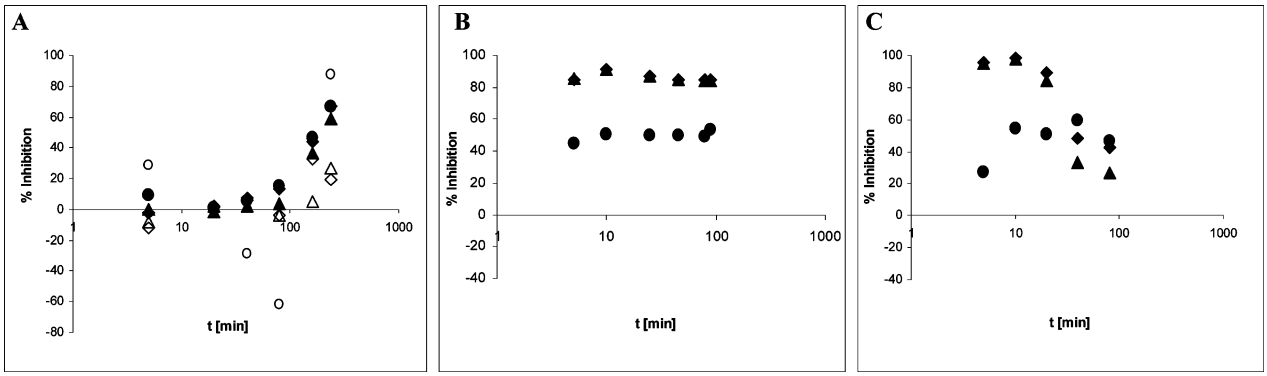

FIGURE 2. Time course in the inhibition of photosynthetic fluorescence quenching for (A) PNA, (B) atrazine, and (C) CCCP; Diamonds, photosynthetic yield; triangles, photochemical quenching; circles, non-photochemical quenching; concentrations: (A) filled symbols 320 μg/L PNA, open symbols 160 μg/L PNA; (B) 100 μg/L atrazine; (C) 500 μg/L CCCP.

as a secondary electron acceptor A in photosystem I in plants and algae (*32*). PNA might, therefore, be expected to interfere with the availability and function of this link of the photosynthetic electron transport chain, though other quinones such as plastoquinone are known to replace phylloquinone.

For the experiments, again, dilution series at different exposure times were run prior to following the time-course of effects at a fixed concentration. In order to interpret possible effect patterns more stringently, two reference compounds were studied in parallel experiments. For one, atrazine, a known inhibitor of the reaction center II processes through competitive binding, and therefore, blockage of electron transfer at the site of plastoquinone (*33*), was selected. Second, CCCP (carbonylcyanide-*m*-chlorophenyl hydrazone) a known decoupler of electron transport and proton-driven ATP-production was used (*34*). Both compounds were expected to alter photosynthetic fluorescence properties but with distinguishable patterns. Figure 2 provides the summarized results of this series of experiments. Shown are the normalized effects detected in *S. vacuolatu*s exposed to 320 and 160 μg/L PNA (A), 100 μg/L atrazine (B), and 500 μg/L CCCP (C) in the time interval 5−120 min and for the fluorescence quenching derived parameters photosynthetic yield (diamonds), photochemical quenching (qP) (triangles), and non-photochemical quenching (NPQ) (circles). Similar to the findings for the photosynthetic oxygen production, PNA demonstrated detectable effects only after a time delay of more than 100 min. The elucidated inhibition is concentration-dependent and similar in degree for all observation parameters. This clearly contrasts with the effects found for atrazine and CCCP which demonstrated immediate effects for the given time resolution of 5 min and distinct patterns for the different fluorescence parameters, consistent with the anticipated mode of actions. Due to their similar water solubility and from further reference compound data, it also seems unlikely, that the delayed response is completely due to a slow pharmacokinetics for PNA.

Pharmacokinetic−Pharmacodynamic Modeling. The observed time-delayed effects prompted a further series of experiments by which the time course of PNA effects on photoautotrophic growth as a susceptible process was investigated. To this end, dilution series of PNA were applied to synchronously growing *S. vacuolatus* cultures and the cell volume distributions of aliquot samples were determined at different cumulated exposure times. The individual cell volume of a *S. vacuolatus* cell increases from 20 to 200 μm^3 on average during a growth period of 14 h. It does not, however, follow a simple exponential function, which excludes an analysis based on growth rates. Cell volume distributions were aggregated to a mean cell volume and then used to calculate a cell volume increase as basis for effects calculation

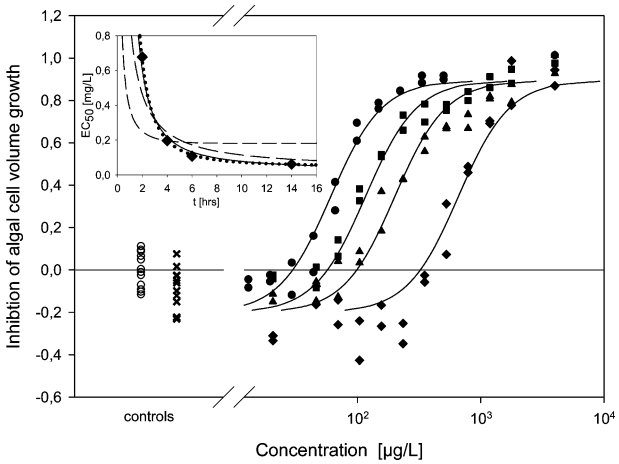

FIGURE 3. Inhibition of increase in the median volume of *Scenedesmus vacuolatus* cells by PNA after different times of cumulated exposure; circles, 14 h; squares, 6 h; triangles, 4 h; diamonds 2 h. Lines represent the five parameter concentration-time-effect model; open circles, negative controls; crosses, co-solvent controls. The inset shows the time-dependent median effects on algal growth as modeled by cirtical body burden, critical target occupation, and a modification of Haber's rule; with diamonds, observed EC_{50} values inhibition of algal volume growth after different exposure duration; dashed lines, predicted time course using critical body burden model with different input constants; full line, predicted time course using whole body critical target occupation model; dotted line, predicted time course using a modification of Haber's rule.

normalized to controls. Results are shown in Figure 3, displaying, apart from the observed effects for different concentration-time treatments, a nonlinear concentration-time-response model fitted to the data. The observed cumulated exposure times were 2, 4, 6, and 14 h, thus covering the whole growth period. Evidently, observed effects in contrast to integrated organism viability responses reported above do not scale between 0 and 100%, but growth increase at low concentrations occurred and growth inhibition leveled out below 100% at high concentration. The structural model, therefore, needed two parameters in addition to slope and activity to account for this. Moreover, in order to capture the time delay of the effect of interest, rather than just fitting four independent concentration effect models for the different cumulative exposure times resulting in 16 parameters to estimate, global fitting of parameters and replacement of individual parameters by time functions were carried out using the SAS NLIN procedure in modification of a generalized version of Haber's rule (*35*, *36*). This resulted in a global model for the observed concentration-time-effect relationship of the following form (eq 1):

$$E(c,t) = \theta_4 + \frac{(\theta_3 - \theta_4)}{1 + \left[\text{conc}/\left(\theta_1 + \frac{\theta_2}{\text{time}^2}\right)\right]^{-\theta_5}} \quad (1)$$

with E, the fractional effect as a function of concentration (conc, in mg/L) and cumulated exposure time (time, in hrs) and the following parameter estimates (standard errors in brackets): incipient EC_{50}, $\theta_1 = 0.0481$ (± 0.0042); Haber's constant, $\theta_2 = 2.44$ (± 0.16); maximal effect, $\theta_3 = 0.894$ (± 0.022); minimal effect, $\theta_4 = -0.203$ (± 0.026); slope, $\theta_5 = 2.09$ (± 0.19).

Equation 1 represents a modified Hill-type function comprising of five parameters whereby the parameter for effectiveness has been replaced by a nested two parameter regression model for the time shift of the median effect. Parameter θ_1 is an expression for the effect concentration at infinite time, while θ_2 would be equivalent to the constant of the Haber equation. As can be deduced from Figure 3, this global model assuming common values for slope, minimum, and maximum effect and allowing only the efficacy to vary with cumulated exposure time already reasonably describes the 92 observations. Only at the shortest exposure time investigated, for the lower concentrations an obvious deviation from the model occurs. The approximate standard error for the parameter estimates also shows the good fit and overall performance of this model. It is interesting to note that this implies the slope of the concentration effect curve does not change with cumulated exposure time. Changes in slope are often considered as indications for alterations in the response sensitivity distribution (*36*). Inhibition of cellular growth can be demonstrated to be in the same effective range (EC_{50} at infinite time estimated as 48 μg/L) as the inhibition of a cell division after 24 h of exposure (EC_{50} 33 μg/L), thus making a specific disturbance of reproductive processes such as DNA replication or cell division at later stages of the cell cycle highly unlikely as a primary cause of PNA phytotoxicity. It is also evident, however, that no immediate interaction, i.e., within a few minutes of exposure, such as a photosystem II inhibition or a protonophore-type activity, would be sufficient to explain the time-delayed response and the apparent pattern of cumulated effects in algae. This might be attributed to pharmacokinetic rather than pharmacodynamic properties of the compound, however.

In a subsequent step to unravel the mode of action of PNA in algae, and possibly plants, the concentration-time-effect data for the inhibition of cell volume growth was modeled using specific pharmacokinetic and pharmacodynamic (PKPD) assumptions. For unspecifically acting organic compounds, it has been suggested that only the final concentration reached within a body or target tissue is responsible for observed effects. This concept, known as critical body burden, can be used to estimate the time-response relationship based on the parameters lethal body burden, the bioconcentration factor (BCF) and the elimination constant (k_2), or alternatively, the effect concentration at infinite time ($EC_{50}(\infty)$) and k_2 (*20*). For the critical body burden model, the fitting was performed again using all 92 observations by replacing the term $\theta_1 + \theta_2/time^2$ in eq 1, which describes the time-dependent shift in median efficacy for $EC_{50}(t)$, so that the concentration-time response model (eq. 2) now reads

$$E(c,t) = \theta_4 + \frac{(\theta_3 - \theta_4)}{1 + \left[\text{conc}/\frac{EC_{50}(\infty)}{[1 - e^{-k_2 t}]}\right]^{-\theta_5}} \quad (2)$$

Parameters are abbreviated as before, using an $EC_{50}(\infty)$ of 48 μg/L as derived from eq 1 for infinite exposure times. Alternatively, k_2 was fixed to 0.646 (hrs^{-1}) and $EC_{50}(\infty)$ estimated as additional parameter (based on ref *37*, see Supporting Information).

Similarly, for an alternative PKPD assumption, namely for the case of irreversibly acting compounds, the time-dependent effect may be attributed to the area under the internal time−concentration curve (CAUC), the BCF and k_2. This model has been termed critical target occupation model (*21*). Due to the high lipophilicity of PNA we employed the whole body critical target occupation model. Again, the time dependent shift in median efficacy ($EC_{50}(t)$) had to be built into the Hill model which, therefore, gives the following (eq 3):

$$E(c,t) = \theta_4 + \frac{(\theta_3 - \theta_4)}{1 + \left(\text{conc}/\left[\frac{\text{CAUC}_{wb}}{\text{BCF}[t - {}^{(1-e^{-k_2 t})}/_{k_2}]} + EC_{50}(\infty)\right]\right)^{-\theta_5}} \quad (3)$$

Parameters are abbreviated as before, whereby the BCF was derived from the K_{ow} using BcfWin version 2.15 (*10*), $EC_{50}(\infty)$ was used as before, and $CAUC_{wb}$ and k_2 were the estimated parameters. Alternatively, we fixed k_2 as explained before and estimated the ratio of $CAUC_{wb}$/BCF and $EC_{50}(\infty)$ as two

TABLE 2. Concentration Time Effect Models and Fitted Parameters for the Inhibition of synchronized Cell Volume of *S. vacuolatus* under Cumulative Exposure with *N*-Phenyl-2-Naphthylamine[a]

		parameter estimates										
model	input constants	θ_1 [SE]	skew	θ_2; [SE]	skew	θ_3, [SE]	skew	θ_4, [SE]	skew	θ_5, [SE]	skew	AIC_c
modified Hill model		0.0481 [0.0042]	0.186	244 [0.16]	0.154	0.894 [0.022]	0.305	−0.203 [0.026]	0.138	2.09 [0.19]	−0.157	−437
critical body burden	EC_{50}(inf), 0.048	fixed		0.0544[b] [0.0053]	0.343	0.936 [0.041]	0.315	−0.171 [0.042]	−0.334	1.86 [0.27]	0.438	−386
critical body burden	k_2, 0.646	0.182 [0.048]	0.539	fixed		0.972 [0.119]	1.356	−0.219 [0.138]	−1.634	1.14 [0.38]	0.393	−256
critical target occupation	k_2, 0.646	0.0172 [0.0052]	0.136	0.516[c] [0.036]	0.165	0.903 [0.024]	0.165	−0.200 [0.028]	−0.183	2.03 [0.20]	0.323	−423

[a] SE, standard error; θ_1 EC_{50}, at infinite time in mg/L; Skewness parameter estimated in SAS proc. NLIN; θ_3, maximal fractional effect; θ_4, minimal fractional effect; θ_5, slope; EC_{50}, expressed in mg/L; k_2, expressed in h^{-1} from ref *27*; k_2, estimate; $CAUC_{wb}$/BCF, estimate; AIC_c, corrected Akaike information criterion.

additional parameters in the nonlinear regression. The joint PKPD model was used with nonlinear regression for fitting all 92 observations. The former approach did not lead to stable parameter estimates for our data when the k_2 was restrained to stay greater 0, while the latter approach converged and produced reasonable parameter estimates.

Table 2 provides the parameter estimates for the different models with error estimates, skewness, and Akaike information criterion, AIC_c, to characterize and compare the different nonlinear model approaches. The parameter θ_1 is the EC_{50} at infinite time, $\theta_{3,4,5}$ represent maximal and minimal fractional effect and the slope of the concentration effect functions, while the meaning of θ_2 is model specific. The actual estimates for $\theta_{3,4,5}$ are pretty similar for the different models which shows that all data are used to drive the functions. The skew measure indicates that the models vary greatly in their ability to fit the observations, as Skew values greater than ± 0.25 indicate apparent nonlinearity and greater than ± 1 indicate that there is considerable nonlinearity in the parameter (*19*). While the former indicates only problems with the parameter estimates, the Akaike information criterion (AIC_c) allows direct comparison between the models (*38*). The lower the AICc value, the better the goodness of fit of a model. While the critical target occupation model achieves an AIC_c value similar to the empirical modified Hill model, the critical body burden model is clearly less well capturing the data.

The inset of Figure 3 displays these findings by using the models to simulate the time dependence of the EC_{50}. The good fit of the critical target occupation model as opposed to the model of critical body burden suggests that, indeed, irreversible activity may explain the time course of the observed effects better than the assumption of an internal critical threshold. One may think of this not only as irreversible receptor binding, which should lead to short-term visible effects, but also in terms of continuously formed reactants (*21*) that cumulatively lead to damage. Also, the tendency that k_2-values which were estimated to be substantially lower than those deduced from ref *37* greatly improved the fitting capabilities of the critical body burden model, point to a possible role of elimination mechanisms in understanding PNA phytotoxicity.

From the results in different organism biotests shown above we conclude that N-phenyl-2-naphthylamine exhibits properties that lead to high phytotoxicity, which seem most prominent for PNA but may be relevant for derivatives also. Our investigation did not reveal a single target or plant-specific process as specifically susceptible to PNA exposure. Rather, primary photosynthetic reactions and subsequently growth and reproduction cease slowly with time and fast with an increase in concentration. Tentatively, we think of it as a reactive toxicity exhibited by PNA, leading to irreversible and thus cumulative damage. In mammals, PNA is reported to be metabolized to epoxides and hydroxylated derivatives as well as N-dephenylated to the carcinogenic compound 2-naphthylamine. The metabolism is catalyzed by the cytochrome system and the prostaglandin endoperoxide synthetase (*39*). The metabolites are known to attack nucleophilic biomolecules such as DNA and proteins (*40*). Due to its high lipophilicity, the intracellular distribution of PNA will be favored in membranes, and therefore, first effects like those observed for photosynthetic reactions might be expected to occur in membrane-rich compartments such as the algal chloroplast. If this holds, distinguishable responses for various parameters in different organisms might depend on a species capacity to metabolize the original compound into less toxic ones or to repair damaged cellular components and functions. Whether this actually happens should be checked in bioassays using prolonged analytically monitored exposure.

Acknowledgments

R.A. acknowledges the receipt of an OECD research fellowship to Roswell Park Cancer Institute, Buffalo. For constructive criticism, we thank three anonymous reviewers. For skillful technical support, thanks are due to Silke Aulhorn, Iris Christmann, and Janet Krueger.

Supporting Information Available

A summary of basic properties of the PNA derivatives investigated, a more detailed description of the bioassays used, and a figure displaying the findings on effect modification with different co-exposure to UV light. This material is available free of charge via the Internet at http://pubs.acs.org.

Literature Cited

(1) Brack, W.; Altenburger, R.; Ensenbach, U.; Möder, M.; Segner, H.; Schüürmann, G. Bioassay-directed identification of organic toxicants in river sediment in the industrial region of Bitterfeld (Germany) - A contribution to hazard assessment. *Arch. Environ. Contam. Toxicol.* **1999**, *37*, 164−174.

(2) Winder, C.; Balouet, J. -C. The toxicity of commercial jet oils. *Environ. Res. A.* **2002**, *89*, 146−164.

(3) BUA (Beratergremium fuer umweltrelevante Altstoffe (BUA) der Gesellschaft Deutscher Chemiker). *N-Phenyl-1-naphthylamin*; S.Hirzel Wissenschaftliche Verlagsgesellschaft, Stuttgart: 1993; p 84.

(4) Jungclaus, G. A.; Lopez-Avila, V.; Hites, R. A. Organic Compounds in an Industrial Wastewater: A Case Study of Their Environmental Impact. *Environ. Sci. Technol.* **1978**, *12*, 88−96.

(5) Lopez-Avilla, V.; Hites, R. A. Organic compounds in an industrial wastewater. Their transport into sediments. *Environ. Sci. Technol.* **1980**, *14*, 1382−1390.

(6) IPCS (international Programme on Chemical Safety) *N-Phenyl-1-Naphthylamine*; WHO: Geneva, 1998.

(7) Wang, H.; Wang, D.; Dzeng, R. Carcinogenicity of N-phenyl-1-naphthylamine and N-phenyl-2-naphthylamine in mice. *Cancer Res.* **1984**, *44*, 3098−3100.

(8) Greenhouse, G. A. Toxicity of N-phenyl-α-naphthylamine and hydrazine to *Xenopus laevis* Embryos and Larvae. *Bull. Environ. Contam. Toxicol.* **1977**, *18*, 503−511.

(9) Altenburger, R.; Walter, H.; Grote, M. What contributes to the combined effect of a complex mixture? *Environ. Sci. Technol.* **2004**, *38*, 6353−6362.

(10) US EPA. EPI Suite V. 3.10, Syracuse Research Cooperation, Syracuse, NY, http://www.epa.gov/oppt/exposure/docs/episuitedl.htm, 2000.

(11) International Organization for Standardization. *Water quality—Determination of the inhibitory effect of water samples on the light emission of Vibrio fischeri (Luminescent bacteria test), Part 1: Method using freshly prepared bacteria*, ISO 11348-1; ISO: Geneva, 1998.

(12) International Organization for Standardization. *Water quality—Determination of the inhibition of the mobility of Daphnia magna Straus (Cladocera, Crustacea)—Acute toxicity test*, ISO 6341; ISO: Geneva, 1996.

(13) Klüttgen, B.; Dülmer, U.; Engels, M.; Ratte, H. T. ADaM, an artificial freshwater for the culture of zooplankton. *Water Res.* **1994**, *28*, 743−746.

(14) Deutsches Institut für Normung e. V. *German standard methods for the examination of water, waste water and sludge—Subanimal testing (group T)—Part 6: Toxicity to fish; Determination of the non-acute-poisonous effect of waste water to fish eggs by dilution limits (T 6)*, DIN 38415-6; DIN: Berlin, 2003.

(15) International Organization for Standardization. *Water quality—Freshwater algal growth inhibition test with unicellular green algae*, ISO 8692; ISO: Geneva, 2004.

(16) Schüürmann, G.; Somashekar, R. K.; Kristen, U. Structure-activity relationships for chloro- and nitrophenol toxicity in the pollen tube growth test. *Environ. Toxicol. Chem.* **1996**, *15*, 1702−1708.

(17) Jung, K.; Kaletta, K.; Segner, H.; Schüurmann, G. ^{15}N Metabolic test for the determination of phytotoxic effects of chemicals and contaminated environmental samples. *Environ. Sci. Pollut. Res.* **1999**, *6*, 72−76.

(18) Scholze, M.; Boedeker, W.; Faust, M.; Backhaus, T.; Altenburger, R.; Grimme, L.H. A general best-fit method for concentration-response curves and the estimation of low-effect concentrations. *Environ. Toxicol Chem.* **2001**, *20*, 448−457.

(19) SAS. *SAS/STAT User's Guide*, V. 8; SAS Institute Inc.: Cary, NC, 1999; p 3884.

(20) Mackay, D.; Puig H.; McCarty, D. An equation describing the time course and variability in uptake and toxicity of narcotic chemicals to fish. *Environ. Toxicol. Chem.* **1992**, *11*, 941−951.
(21) Legierse, K. C. H. M.; Verhaar, H. J. M.; Vaes, W. H. J.; de Bruijn, J. H. M.; Hermens, J. L. M. Analysis of the time-dependent acute aquatic toxicity of organophosphorus pesticides: The critical target occupation model. *Environ. Sci. Technol.* **1999**, *33*, 917−925.
(22) Escher, B. I.; Hermens, J. L. M. Modes of action in ecotoxicology: Their role in body burdens, species sensitivity, QSARs, and mixture effects. *Environ. Sci. Technol.* **2002**, *36*, 4201−4217.
(23) Lipnick, R. L. Outliers: their origin and use in the classification of molecular mechanisms of toxicity. *Sci. Total Environ.* **1991**, 109−110, 131−153.
(24) VanWezel, A. P.; Opperhuizen, A. Narcosis due to environmental pollutants in aquatic organisms, residue-based toxicity, mechanisms, and membrane burdens. *Critical Rev. Toxicol.* **1995**. *25*, 255−279.
(25) Niederlehner, B. R.; Cairns, J., Jr; Smith E. P. Modeling acute and chronic toxicity of nonpolar narcotic chemicals and mixtures to Ceriodaphnia dubia. *Ecotoxicol. Environ. Saf.* **1998**, *39*, 136−146.
(26) Hermens, J.; Busser, F.; Leeuwangh, P.; Musch, A. Quantitative structure-activity relationships and mixture toxicity of organic chemicals in *Photobacterium phosphoreum*: the Microtox test. *Ecotoxicol. Environ. Saf.* **1985**, *9*, 17−25.
(27) Pavan, M.; Worth, A.; Netzeva, T. *Preliminary analysis of an aquatic toxicity dataset and assessment of QSAR models for narcosis*, EUR 21749; IHCP, JRC: Ispra, Italy, 2005.
(28) Brack, W.; Altenburger, R.; Küster, E.; Meissner, B.; Wenzel, K.-D.; Schüürmann, G. Effect-directed identification of toxic products of anthracene photomodification in simulated sunlight. *Environ. Toxicol. Chem.* **2003**, *22*, 2228−2237.
(29) Grote, M.; Schüürmann, G.; Altenburger, R. Modelling photo-induced algal toxicity of polycyclic aromatic hydrocarbons. *Environ. Sci. Technol.* **2005**, *39*, 4141−4129.
(30) Kromkamp, J. C.; Forster, R. M. The use of variable fluorescence measurements in aquatic ecosystems: differences between multiple and single turnover measuring protocols and suggested terminology. *Eur. J. Phycol.* **2003**, *38*, 103−112.
(31) Dwivedi, P, C.; Rao, K. G. Electron donor-acceptor complexes of N-phenyl-2-naphthylamine with quinones. *Indian J. Chem.* **1972**, *10*, 944−945.
(32) Leonova, N. M.; Zhukova, E. E.; Evstigneeva, R. P. A model of the quinone-binding site of photosystem I: Investigation of charge transfer complexes of phylloquinone and its derivatives with tryptophan. *Biofizika.* **2004**, *49*, 970−978.
(33) Copping, L. G.; Hewitt, H. G. *Chemistry and mode of action of crop protection agents*; RSC Publishing: Cambridge, 1998.
(34) Popova, L. G.; Shumkova, G. A.; Andreev, I. M.; Balnokin, Y. V. Functional identification of electrogenic Na^+-translocating ATPase in the plasma membrane of the halotolerant microalga *Dunaliella maritima*. *FEBS Lett.* **2005**, *579*, 5002−5006.
(35) Bunce, N. J.; Remillard, R. B. J. Haber's rule: The search for quantitative relationships in toxicology. *Human Ecol Risk Assess.* **2003**, *9*, 973−985.
(36) Levasseur, L. M.; Slocum, H. K.; Rustum, Y. M.; Greco, W. R. Modeling of the time-dependency of in vitro drug cytotoxicity and resistance. *Cancer Res.* **1998**, *58*, 5749−5761.
(37) Sijm, D. T. H. M.; Broersen, K. W.; de Roode, D. F.; Mayer, P. Bioconcentration kinetics of hydrophobic chemicals in different densities of Chlorella pyrenoidosa. *Environ. Toxicol. Chem.* **1998**, *17*, 1695−1704.
(38) Ludden, T. M.; Beal, S. L.; Sheiner, L. B. Comparison of Akaike Informaation Criterion, the Schwartz Criterion and the F Test as Guides to Model selection. *J Pharmacokinet. Biopharm.* **1994**, *22*, 431−445.
(39) Laham, S.; Potvin, M. Comparative N-dephenylation of N-phenyl-2-naphthylamine in sprague-dawley rats and New Zealand white rabbits. *Chemosphere* **1984**, *13*, 657−667.
(40) Anderson, M. M.; Mitchum, R. K.; Beland, F. A. Hepatic microsomal metabolism and macromolecular binding of the antioxidant, N-phenyl-2-naphthylamine. *Xenobiotica* **1982**, *12*, 31−43.

Received for review February 14, 2006. Revised manuscript received July 19, 2006. Accepted July 25, 2006.

ES060338E